Building Tomorrow's Society
Bâtir la Société de Demain

Fredericton, Canada
June 13 – June 16, 2018/ *Juin 13 – Juin 16, 2018*

INVESTIGATION OF DISCHARGE COEFFICIENT FOR SIPHON SPILLWAY

Ahmed, Warda[1,4], Li, S. Samuel[2] and Ramamurthy, Amruthur [3]
[1] *Department of Building, Civil & Environmental Engineering, Concordia University,* Canada
[2] *Department of Building, Civil & Environmental Engineering, Concordia University,* Canada
[3] *Department of Building, Civil & Environmental Engineering, Concordia University,* Canada
[4] wa_ah@encs.concordia.ca

Abstract: Flow control is an important application of hydraulic engineering. For this purpose, a siphon spillway is attractive because of its great ability to pass full discharge with a minimum increase in the upstream head. In fact, siphon spillways have been extensively used as an efficient flow-control structure in open-channel systems. The proper design of siphon spillways requires reliable estimates of the relationship between discharge and the difference in water levels on the upstream and downstream sides. Such relationship involves a discharge coefficient. This is a key parameter for the design of functional siphon spillways. The purpose of this paper is to investigate the discharge coefficients under the conditions of submerged water flow at the outlet of a siphon passage. Siphon discharges under submerged conditions have not been thoroughly investigated in the past. This paper takes the approach of combing computational fluid dynamics (CFD) with laboratory experiments. Computations of the two-phase flow field and pressure distributions have been performed for a range of values for the Reynolds number. A physical model of siphon spillway has been fabricated and tested in the Water Resources Laboratory at Concordia University. These laboratory measurements are used to determine the experimental values for the discharge coefficient. The dependence of the discharge coefficient on the dimensionless head is predicted through computational fluid dynamics (CFD) modelling. The experimental results are used to validate the model predictions. The predictions agree well with the experimental data.

Keywords: Siphon spillway; discharge coefficient, internal flow structure, laboratory measurements, CFD predictions, two-phase flow.

1 INTRODUCTION

The control of flow in open channels is one of the important issues in hydraulic engineering. Various types of spillways for flow control may be used to release an excessive amount of water from a reservoir, when it is necessary, in order to protect the reservoir and the surrounding areas. Also, it is a good practice to keep the reservoir water level low before floods occur (Linsley and Franzini 1971). In some cases, hydraulic structures regulate the flow in the systems and pass water to canals or pipelines. A siphon spillway is a flow regulation structure for the control of open channel flow. Siphon spillway consists of a closed U-shaped conduit system. Its cross-section can be rectangular or circular. As the water level in the reservoir rises above the crest, the incoming flow is discharged like the flow over a weir (free flow). Siphon priming occurs when the water level rises and the air from the downstream cannot access the conduit (Head 1971). Based on experimental results and simplified theoretical considerations, the initial flow discharge can be expressed as:

[1] $q = \frac{2}{3} Cd\ b\ 2g^{\frac{1}{2}} h^{\frac{3}{2}}$

where q is the flow rate (m^3/s), h is the head on the weir (m), b is the width of the weir (m), g is the gravity, and C_d is the discharge coefficient (Chow 1959). When the siphonic action occurs and the siphon acts as a pipe, the flow discharge will be:

[2] $q = Cd\sqrt{2g\Delta H}$ (2)

where $\Delta H = H_1 - H_2$; H_1 and H_2 are the heads of water upstream and downstream, respectively. The siphon spillway has superb hydraulic characteristics such as:

- Relatively large discharge capacity and a narrow range of upstream water level;
- No moving components.

Flow through the siphon spillway can pass with free surface or under pressure state. In the free surface condition, the siphon acts as a weir. In contrast, in the under-pressure condition, it acts as an orifice. The analysis of the mean characteristics of curvilinear flow in a spillway is an important problem. With rapid development in computational hydraulics to help solve the equations that govern fluid flow, engineers now must decide which method(s) to use to evaluate existing and proposed spillway designs. Many studies have provided information about siphon spillways, including definitions and descriptions of siphons. Head (1971) investigated an air–regulated siphon and described its design and operation. Subsequently, Head (1975) experimentally studied a low-head-regulated siphon. Savage and Johnson (2001) studied the flow over an Ogee spillway experimentally and numerically. The main purposes of their studies were to compare their experimental and numerical results with the existing results from the U.S. Bureau of Reclamation's (USBR, 1977) and the U.S. Army Corps of Engineers' (USACE, 1990) design reports. Babaeyan-Koopaei et al. (2002) presented a case study on the hydraulic performance of the Brent reservoir siphon spillway. More recently, a few numerical studies have also been reported. For instance, Tadayon and Ramamurthy (2013) used the RNG k-ε model to obtain the coefficient of discharge for a siphon spillway. They validated their model predictions using results of experiments related to a physical model of the siphon spillway.

2 PHYSICAL MODEL

The physical model is an incomparable tool of communication; it provides a three-dimensional and complete overall appreciation of project and facilitates the explanation of the hydraulic phenomena. The experiments were carried out using a recirculation flume and a physical model of a siphon spillway was fabricated and tested in the Water Resources Laboratory at Concordia University (Figure 1). Plexiglas was used to fabricate and construct the physical model. Plexiglas is chosen because it is easy to form into shape and can produce smooth curves. The sidewalls were made of Plexiglas plates for flow visualization. The Plexiglas siphon spillway model was inserted into a rectangular flume of width b = 30 cm and height 65 cm to determine the coefficient of discharge through the siphon over a range of Reynolds numbers. The siphon sections were 25.1 cm wide and 5.74 cm deep. The radii of the crest and crown were, respectively, 1.83 cm and 7.4 cm. The model also included a tangent section and a rectangular exit. From previous studies, it is clear that the shape of the entrance, the geometry of the outlet, the depth of water downstream, and the size and position of the deflector can influence the siphon discharge coefficient, C_d. For this reason, it is important to take these variables into account and verify the configuration of the entrance, crest radius, deflector shape and position, and outlet geometry.

2.1 Setup of the Flume

Tests were performed on the spillway model with different combinations of upstream and downstream water levels. The upstream and downstream water levels were measured using accurate point gauges (±0.1 mm). Flow rates were measured using a standard 60° V-notch. Pressure was recorded using a sufficient number

of pressure taps of 0.5 mm in diameter, which were attached to the physical model of the siphon. The pressure taps recorded the pressure distributions along the centreline of the model, on the spillway crest and crown. Siphon discharge was calculated by measuring discharge flow rate using the hydraulic head, determined by surveying the elevation difference between the free water surface upstream and downstream.

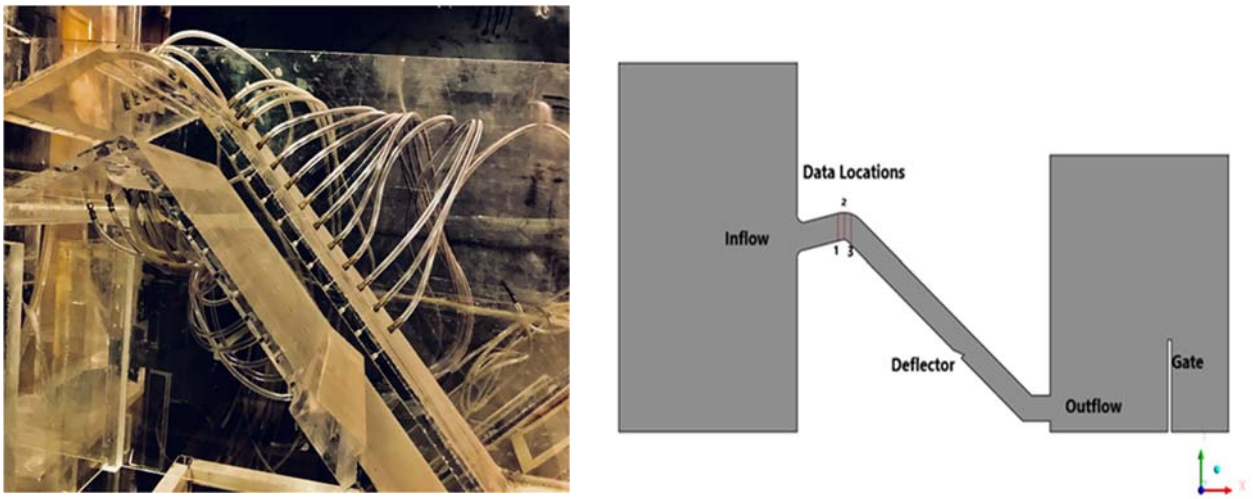

(a) (b)

Figure 1: A photo of the physical model of the siphon (panel a), and longitudinal section of the siphon spillway (panel b).

2.2 Experimental conditions

A control valve was used to set the flow in the model and change the flow rate. $\triangle H/d$ ranged from 2.5 to 7 (Table 1). Here, $\triangle H$ is the difference between water depth upstream and downstream and d is the water depth at the crest section. For all test cases, the downstream water level was kept higher than the outlet level using a tail gate to ensure that the flow downstream is submerged.

Table 1: A summary of hydraulic conditions for the siphon experiments.

Flow rate (m^3/s)	upstream water level (m)	Downstream water level (m)	Dimensionless head ($\Delta H/d$)	Discharge coefficient (C_d)
0.024	0.565	0.203	6.351	0.637
0.025	0.557	0.228	5.767	0.676
0.024	0.518	0.156	6.353	0.637
0.022	0.569	0.26	5.435	0.623
0.024	0.612	0.275	5.919	0.646
0.024	0.577	0.225	6.177	0.648

3 COMPUTATIONAL MODEL

3.1 Governing Equations

In open channels, almost all the flows countered are turbulent flow. Turbulent flow is naturally unsteady, rotational, and three-dimensional. Computational fluid dynamics (CFD) allows us to examine flow behaviour

in hydraulic structures within reasonable time and expense constraints. A three-dimensional geometry to modelling the flow on the siphon spillway was reproduced using Fluent 18.1 software. The Reynolds-averaged Navier-Stokes (RANS) equations were used to solve the problems of flow through a siphon spillway with a rectangular open channel.

Assume that the flow of water in open channels is Newtonian and incompressible. The Reynolds-averaged equations for the conservation of mass and momentum equations are given by:

[3] $\frac{\partial u_i}{\partial x_i} = 0$

[4] $\frac{\partial u_i}{\partial t} + u_j \frac{\partial u_i}{\partial x_i} = -\frac{1}{\rho}\frac{\partial P}{\partial x_i} + \frac{\partial}{\partial x_j}(2\nu S_{ij} + \tau_{ji})$

where ρ, v, t, and x_i are the density of water, kinematic viscosity of water, time, and Cartesian coordinates (i = 1, 2,3), respectively; u_i is the Reynolds-averaged velocity component in the x_i-direction; p is the Reynolds-averaged pressure (Ferziger 2002). The Reynolds-stress tensor, τ_{ij}, and the strain-rate tensor, S_{ij}, are defined as follows:

[5] $S_{ij} = \frac{1}{2}(\frac{\partial u_i}{\partial x_j} + \frac{\partial u_j}{\partial x_i})$

[6] $\tau_{ij} = -\overline{u_i' u_j'}$

where u_i' is the fluctuating part of velocity. Based on the Bousssinesq approximation, the components of the Reynolds stress tensor vary linearly with the mean rate of strain tensor, which can be written as follows:

[7] $\tau_{ij} = 2\nu_T S_{ij} - \frac{2}{3}k\delta_{ij}$

where ν_T is the kinematic eddy viscosity; k is the turbulence kinetic energy; and δ_{ij} is the Kronecker symbol (δ_{ij} = 1 if i = j and δ_{ij} = 0 otherwise).

The RNG k-ε model predicts and simulates accurately the characteristics of near-wall boundary flows and flows in curved boundaries. Many previous studies have shown the effectiveness of the RNG k-ε model with high accuracy in flow simulation. Shekari (2015) compared different models (the Reynolds shear stress model, standard k–ε model, RNG k–ε model, and realizable k–ε model) to predict the turbulent flow, and the author concluded that the RNG k-ε model gives the best results. The RNG k-ε model has been properly validated. Tadayon and Ramamurthy (2013) showed that the RNG k-ε model provides the required flow characteristics and discharge coefficient of the water flow through siphon spillways.

This model estimates the kinematic eddy viscosity as follows (Wilcox 2006).

[8] $\nu_T = C_\mu k^2/\varepsilon$

This model expresses the turbulent eddy viscosity in terms of turbulence kinetic energy, k, and dissipation rate of turbulence kinetic energy, ε. The two turbulent quantities are calculated from transport equations:

[9] $\frac{\partial k}{\partial t} + u_j \frac{\partial k}{\partial x_j} = \tau_{ji}\frac{\partial u_i}{\partial x_j} - \varepsilon + \frac{\partial}{\partial x_j}[\left(\nu + \frac{\nu_T}{\sigma_k}\right)\frac{\partial k}{\partial x_j}]$

[10] $\frac{\partial \varepsilon}{\partial t} + u_j \frac{\partial \varepsilon}{\partial x_j} = C_{\varepsilon 1}\frac{\varepsilon}{k}\tau_{ji}\frac{\partial u_i}{\partial x_j} - C_{\varepsilon 2}\frac{\varepsilon^2}{k} + \frac{\partial}{\partial x_j}[\left(\nu + \frac{\nu_T}{\sigma_\varepsilon}\right)\frac{\partial \varepsilon}{\partial x_j}]$

The volume of fluid (VOF) method rests on conceptualization involving a fractional volume of fluid. This method calculates the shape and location of a constant-pressure free surface boundary, according to a filling process which is used to identify which cell in the meshing volume is filled and which is emptied. This is modelled using a volume fraction field, which is equal to one if the cell is completely filled and zero if the cell is completely emptied. Knowing the amount of fluid in each cell allows us to locate the position of the free surface, as well as to model surface slopes and curvatures. The free surface can be easily located through the partially filled cells or between the full and empty cells. Note that u_1, and u, u_2 and v, u_3 and w, are used interchangeably in this paper. Similarly, x_1 and x, x_2 and y, x_3 and z.

3.2 Model Domain

The model domain was meshed with a power law function that generates the finer mesh close to the solid boundaries. The first cell next to a solid boundary was constructed well within the logarithmic region with $30 < y+ < 100$. Figure 1 shows the computational grid in the siphon spillway model. Unstructured mesh was used in different sizing for the mesh development and a fine mesh was used at the area around the crest (Figure 2).

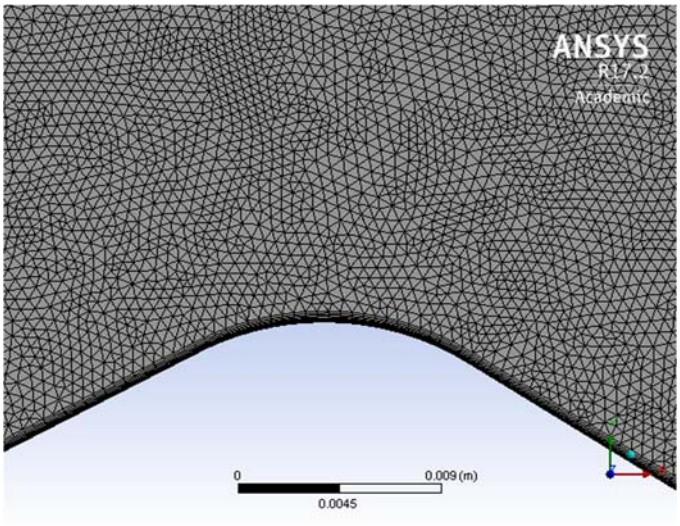

Figure 2. A vertical section shows the grid in the siphon crest.

For flow simulations, it is important that the boundary conditions accurately represent the real prototype and its physical conditions. The conditions at the boundaries (Figure 3) in the numerical model are as follows: a) upstream of the siphon, the left boundary is modeled as a velocity inlet with pressure based on water depth upstream of the siphon; b) at the outlet, downstream of the siphon the boundary is pressure outlet; c) sidewalls and the bottom of the channel are no-slip walls; d) similarly, the boundary condition of the siphon body is no-slip wall. Siphon walls modeled as no slip are defined as zero tangential and normal velocities ($u = v = w = 0$). With a no-slip boundary, it is assumed that the law of the wall profile exists in the boundary region. Since the purpose of these simulations is to model flow over the siphon with deferent water levels, all the air boundaries are defined as pressure boundaries with gauge pressure equal to zero.

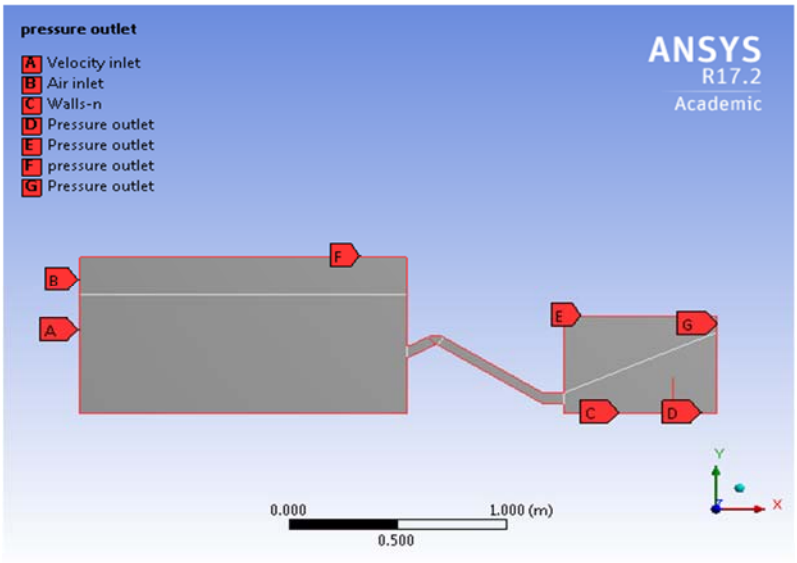

Figure 3. Model domain showing the upstream and downstream reservoirs connected by a siphon.

4 RESULTS

The velocity vectors through the siphon are illustrated in Figure 4. Upstream flow vectors show that the upstream flow is two-dimensional, subcritical flow and the vectors indicate smooth flow toward the siphon inlet. At the siphon inlet, the velocity vectors are contracted toward the flow path. At the crest, velocity vectors are forced to flow in the extrados direction under the impact of the centrifugal force. This force can decrease the distance between the streamlines with high velocity above the crest and low velocity under the crown. The deflector ensures that there are no air bubbles inside the siphon even if the water level in the downstream drops.

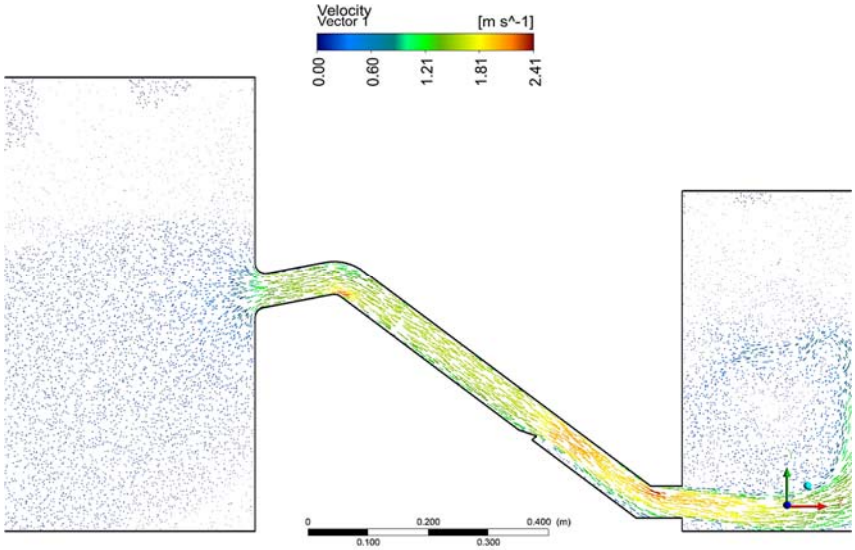

Figure 4. Velocity vectors at the crest.

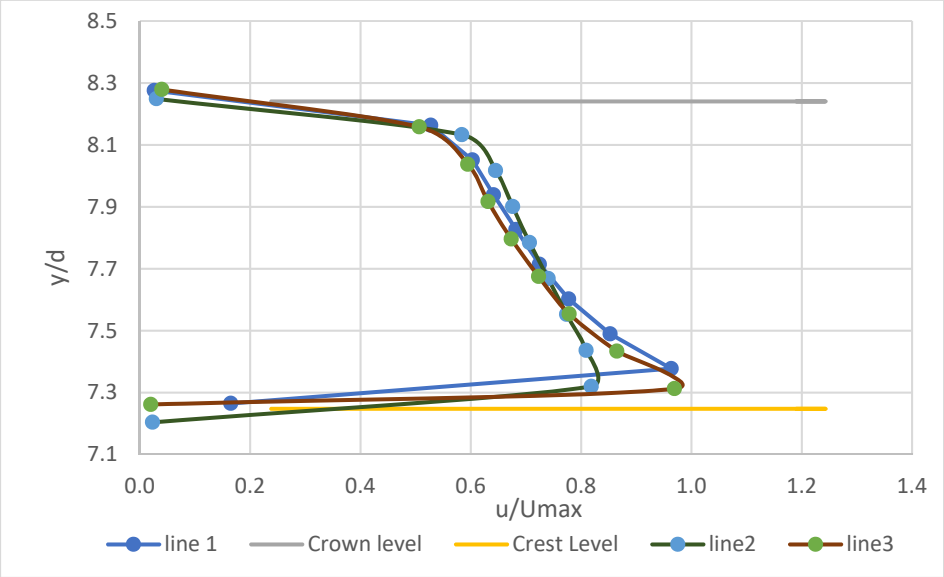

Figure 5. Vertical distribution of the horizontal velocity at the crest section in three different locations.

The horizontal velocity component u was computed at the siphon crest section in three different locations: lines 1, 2 and 3 as marked in Figure 1. Line 2 is the centerline of the siphon's crest, line 1 is located upstream of the crest centerline, and line 3 is located downstream of the crest centerline of the siphon crest. Figure 5 shows the comparison between the velocity profiles at lines 1, 2 and 3. The vertical axis is the ratio of the water depth above the crest (y) to the siphon diameter (d), and the horizontal axis is the velocity (u) at the depth (y) normalised by the maximum velocity (U_{max}). Above the crest, the velocity increases rapidly to reach the maximum value at the edge of the thin boundary layer of thickness δ where δ<< d. Subsequently, the velocity decreases gradually until it becomes a small value approaching zero at 99% of the total water depth approximately.

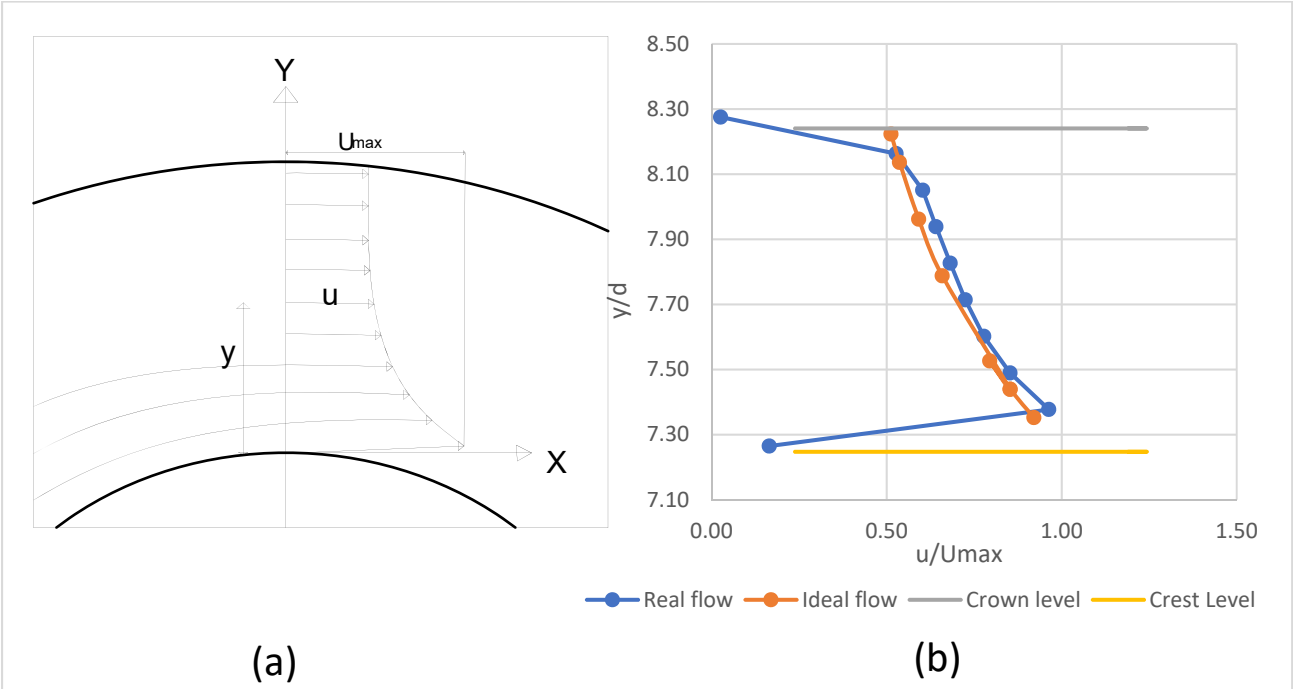

Figure 6. Comparison of computed horizontal velocity and ideal analytical solution profile: (a) potential flow past a cylinder (Vallentine 1967), (b) flow past the siphon crest.

For the purpose of comparison, the ideal flow velocity profile was calculated. The horizontal velocity u at any depth y is expressed as:

[11] $u = \frac{U}{(1+\frac{y}{r})}$

where U is the maximum velocity above the crest, u is the horizontal velocity at the depth y, and r is the crest radius (Dressler 1978). The comparison shows consistencies between the real-fluid flow and the ideal-fluid flow velocity profiles (Figure 6). The velocity in the ideal-fluid flow is the maximum at the crest and decreases steadily with increasing water depth y. By comparing the potential flow profile [Figure 6 (b)], with the potential flow over a cylinder [Figure 6 (a)], both cases have similar flow velocity profile.

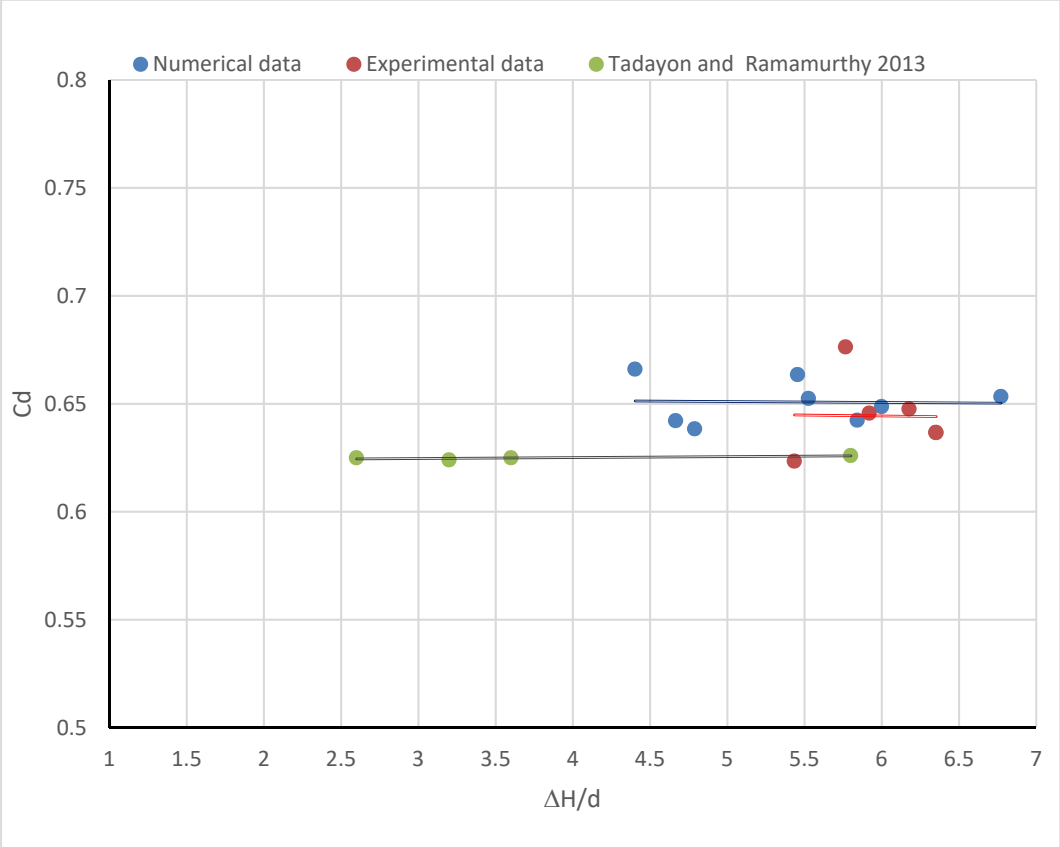

Figure 7. Variation of discharge coefficient.

Figure 7 shows the comparison of the predicted results with the experimental data of C_d. The y- axis indicates discharge coefficient (C_d) and the x-axis is the ratio of the upstream and downstream water levels difference (ΔH) to the water depth at the siphon crest (d). The results were normalised to allow a comparison in their simplest form. The data related to C_d and ΔH/d indicates that, because the effect of viscosity decreases as the Reynolds number increases, the numerical results become much closer to experimental results at higher ΔH/d.

The discharge coefficient in the case of submerged outlet is about 0.63 to 0.66. Also, Figure 7 shows the results of free flow condition from the previous study by Tadayon and Ramamurthy (2013). The discharge coefficient is between 0.62 and 0.63 in the case of free flow, therefore, the trend in both cases is the same.

5 CONCLUSIONS

Because of its great ability to pass the full discharge with a minimum increase of the upstream head, the siphon spillway has been used extensively and efficiently as a flow regulation structure in open channels. The present study has investigated the curvilinear flow over a siphon spillway and the discharge coefficient experimentally and numerically. The horizontal velocity profile over the siphon crest was obtained and compared with the potential flow profile. The velocity reached the maximum value near the crest of the siphon. The discharge coefficient in the case of submerged flow was investigated. The numerical results show that the flow field computed by the RNG k-ε model match well with the measured data.

References

Babaeyan-Koopaei, K, Valentine, E. M. and Ervine, D. A. 2002. Case study on hydraulic performance of Brent reservoir siphon spillway. *Journal of Hydraulic Engineering*, **128**(6): 562-567.

Bruce M. Savage and Michael C, Johnson. 2001. Flow over Ogee spillway: physical and numerical case. *Journal of Hydraulic Engineering*, **127(**8): 640-649.

Chow, V. T. 1959. Open-Channel Hydraulics. McGraw-Hill, Inc., New York.

C. R. Head.1971. A self-regulating river siphon. *Journal of the Institution of Water Engineers*, 25: 63-72

C. R. Head.1975. Low-head air-regulated siphons. *Journal of the Hydraulics Division, ASCE,* **101**(3): 329-345.

Dressler, R.F. 1978. New Nonlinear Flow Equations with Curvature. *Journal of Hydraulic Research, IAHR*, **16**(3): 205-222.

Ferziger, J. H. and Peric, M. 2002. Computational Methods for Fluid Dynamics. 3rd edition, Springer Verlag Berlin Heidelberg.

R. Tadayon, and A. S. Ramamurthy. Discharge Coefficient for Siphon Spillways. 2013. *Journal Irrigation and Drainage Engineering, ASCE,* **139**(3):267-270.

Linsley, R. K. and Franzini, J. B. 1971. “Water-Resources Engineering.” McGraw-Hill, New York.

Savage, B.M. and Johnson, M.C. 2001. Flow over ogee spillway: Physical and numerical model case study. *Journal of Hydraulic Engineering, ASCE,* **127**(8): 640-649.

Shekari, Y., Javan, M., and Eghbalzadeh, A. 2015. Effect of turbulence models on the submerged hydraulic jump simulation. *Journal of Applied Mechanics and Technical Physics*, **56**(3): 454-463

USACE.1990. Hydraulic Design of Spillways. EM 1110-2-1603, Department of the Army, Washington, DC.

USBR 1977. Design of Small Dams. U.S. Government Printing Office, Washington, D.C.

Vallentine R. H. 1967. Applied Hydrodynamics. 2nd edition., London Butterworths, London.

Wilcox, D. C. 2006. Turbulence Modeling for CFD, 3rd edition., DCW Industries, Inc., La Canada, CA.